Delineation and Fine-Scale Structure of Active Fault Zones during the 2014-2023 unrest at the Campi Flegrei Caldera (Southern Italy) from High-Precision Earthquake Locations

***Francesco Scotto di Uccio*[1], *Anthony Lomax*[2], *Jacopo Natale*[3], *Titouan Muzellec*[1], *Gaetano Festa*[1,4], *Sahar Nazeri*[1], *Vincenzo Convertito*[5], *Antonella Bobbio*[5], *Claudio Strumia*[1] and *Aldo Zollo*[1]**

[1] Department of Physics Ettore Pancini, Università di Napoli Federico II, Napoli, Italy

[2] ALomax Scientific, Mouans-Sartoux, France

[3] Department of Earth and Geoenvironmental Sciences, Università di Bari "Aldo Moro", Bari, Italy

[4] Istituto Nazionale di Geofisica e Vulcanologia, Roma, Italy

[5] Osservatorio Vesuviano, Istituto Nazionale di Geofisica e Vulcanologia, Napoli, Italy

Corresponding author: Aldo Zollo (aldo.zollo@unina.it)

Key Points:

- High-precision location of 2014-2023 seismicity in Campi Flegrei images active fault zones with unprecedented detail.
- From 2021 onwards the seismicity produces an elliptic pattern resembling that of the 1982-84 unrest phase of the caldera.
- Seismicity occurs along different volcano-tectonic structures including the inner ring fault zone and faults bounding the Solfatara crater.

Abstract

In the past two decades, the central portion of Campi Flegrei caldera has experienced ground uplift of up to 15 mm/month, and a consequent increase in the rate, magnitudes and extent of seismicity, especially in the last two years. We use a new method for multi-scale precise earthquake location to relocate the 2014-2023 seismicity and map in detail currently activated fault zones. We relate the geometry, extent, and depth of these zones with available structural reconstructions of the caldera. The current seismicity is mainly driven by the time-varying, ground-uplift induced stress concentration on pre-existing, weaker fault zones, not only related to the inner caldera, dome resurgence but also to ancient volcano-tectonic collapses and magma emplacement processes. The extent of imaged fault segments suggests they can accommodate ruptures up to magnitude 5.0, significantly increasing estimates of seismic hazard in the area.

Plain Language Summary

During the past two years, there has been a marked increase of ground uplift and number and size of earthquakes at Campi Flegrei caldera. This increase in activity has raised concerns in the population and public authorities about the impact of seismic activity on buildings and infrastructure in the area and about the best actions to undertake during the seismic emergency to reduce the risk. Additionally, the possibility of a future volcanic eruption is being considered, although currently geochemical and geophysical monitoring shows no clear and unequivocal signs of precursory phenomena. In this work we map the last decade of seismicity with high-precision earthquake locations with the aim of unveiling the currently activated fault zones of the inner caldera and assessing the potential hazard of earthquake ruptures along the delineated fault zone. The results show an expanding, near-elliptical distribution of seismicity. The size of faults imaged in the caldera suggest earthquakes up to magnitude 5.0 can occur, significantly increasing estimates of seismic hazard in the area.

1 Introduction

The Campi Flegrei caldera, in Southern Italy is located nearby the one million people living in wide metropolitan area of Napoli, making it the worldwide most densely urbanized volcanic area (e.g., Charlton et al., 2020). During the past two decades, the central portion of Campi Flegrei caldera experienced a sustained and continuous ground uplift, reaching rates of 15 mm/month,

with a consequent increase of the rate, magnitudes and extent of seismicity, especially in the last two years.

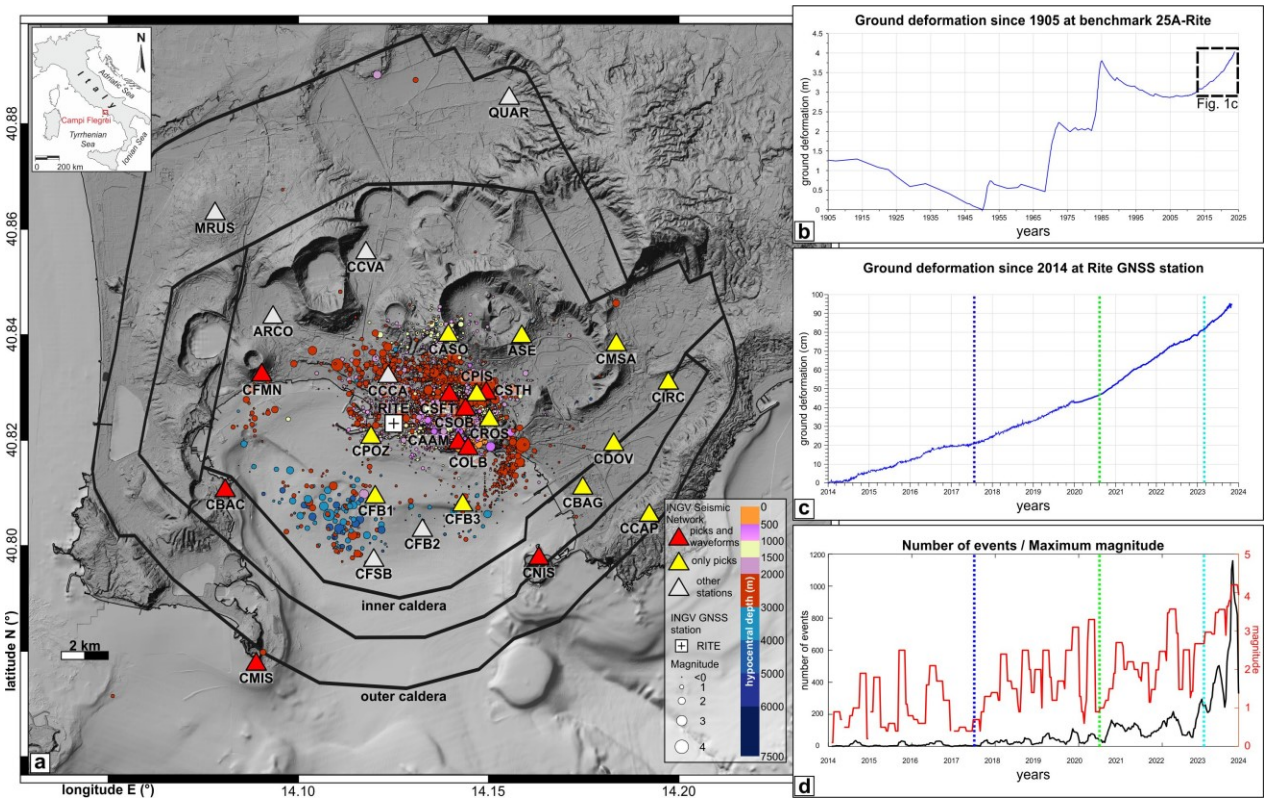

Figure 1. a) Shaded relief map of Campi Flegrei with simplified caldera boundaries (modified after Natale et al., 2022b), showing epicentral locations of the 2014-2023 seismicity recorded by INGV seismic network as retrieved from INGV-Osservatorio Vesuviano bulletin database (https://terremoti.ov.ingv.it/gossip/index.html), color coded by hypocentral depth and scaled by magnitude. Triangles show the location of seismic stations color-coded as follows: red for stations at which both picks and waveforms are available; yellow for stations with only picks available; gray for other INGV stations. White box with black cross shows the location of RITE GNSS station. b) Vertical ground deformation recorded at benchmark 25A and RITE GNSS station since 1905 (modified after Del Gaudio et al., 2010; INGV 2023 Monthly Bulletin), dashed black box shows the extent of Figure 1c. c) Uplift recorded at Rite GNSS station since 2014, vertical dotted lines indicate the occurrence of changes in uplift rate. d) Temporal evolution of number of events and maximum magnitude since 2014 computed in overlapping windows of 60 days with a time shift of 10 days.

Extensive and accurate geophysical and geochemical monitoring is fundamental to understanding and modelling volcanic processes during unrest (Tilling, 2008). Changes in seismicity are usually

main precursors to volcanic eruptions, and are one of the primary indicators of the initiation and evolution of a magmatic intrusion episode (McNutt et al., 1996). Since errors in earthquake locations may preclude clear understanding of the ongoing processes, the use of precise seismicity relocation techniques is emerging as a valuable tool to provide a comprehensive view of activated faults and fractures during volcanic unrest, such as at the Campi Flegrei caldera.

The Campi Flegrei volcano is characterized by a nested caldera structure (Figure 1a; Orsi et al., 1996; Orsi, 2022), produced by two large explosive eruptions, referred to as the Campanian Ignimbrite (CI) and the Neapolitan Yellow Tuff (NYT), at 39 ka and 14.5 ka, respectively (Silleni et al., 2020; Orsi et al., 1992), whose boundaries are now mapped also offshore (Natale et al., 2022b). Since the NYT, over 70 eruptions occurred within the caldera boundaries, clustered in time (i.e., volcanic epochs; Di Vito et al., 1999) and space along the main structural features (e.g., Bevilacqua et al., 2015). Since 10.5 ka, the volcanic activity is remarkably coupled with a caldera resurgence phenomenon broadly acting in the central sector (Natale et al., 2022a), and displaying a bell-shaped deformation pattern regardless of the scale and the polarity (uplift/subsidence). This is similar to what is observed during historical ground deformation episodes (Bevilacqua et al., 2020; Vitale and Natale, 2023).

Volcanic unrest and eruptions in the caldera are accompanied by seismotectonic phenomena. Precursory seismicity and ground deformation patterns preceding the last historical eruption of Monte Nuovo in 1538 CE (Di Vito et al., 2016) are similar to those in the current activity of the caldera (Del Gaudio et al., 2010; Osservatorio Vesuviano – INGV, 2023).

Due to the high volcanic and seismic risk, the Campi Flegrei volcano hosts a highly advanced, permanent multiparametric monitoring system (Bianco et al., 2022), including a dense seismic monitoring network (Figure 1a). A series of ground uplift-subsidence with seismic activity (bradyseismic) episodes affected the central area of Pozzuoli since early 1950s (Del Gaudio et al., 2010), with the two most rapid uplift phases occurred in 1970-72 and 1982-84, reaching a maximum uplift of about 4 m at RITE station in 1984 (Figure 1b), and producing over 20000 shallow earthquakes overall (D'Auria et al., 2011), concentrated in the Solfatara-Pisciarelli area (Isaia et al., 2021). A long subsidence phase occurred between 1985 and 2005, with a maximum subsidence of 90 cm and relatively rare seismicity (Gaeta et al., 2003). Since 2005 a new, long-term, monotonic uplift phenomenon started with unsteadily accelerating seismicity (Bevilacqua et al., 2022), especially from 2014 onwards (Figure 1c), which has produced a clear increase in the

number of seismic events and of the maximum magnitude (Figure 1d). At the beginning of 2023 the uplift surpassed the maximum elevation achieved during the previous 1982-1984 crisis (Figure 1b). The cause of the bradyseismic episodes is still debated within the volcanological community (e.g., Troise et al., 2019). The main hypotheses are that the deformation is either directly caused by pressure and/or volume changes induced by magma emplacement and intrusion at shallow depths beneath the caldera (Woo and Kilburn, 2010; Macedonio et al., 2014) or it is due to the poroelastic response of the shallow hydrothermal system to changes in pore pressure and fluid content (Bonasia et al., 1984; Bonafede, 1991; Todesco, 2021; Nespoli et al., 2023). The latter could be driven by the periodic migration toward the surface of crustal fluids possibly generated by degassing processes at the primary, sill-like magma reservoir detected at 8 km depth by seismic reflection experiments (Zollo et al., 2008). In favor of this second hypothesis, a lack of detectable amount of magma at shallow depths was reported by previous seismic reflection soundings, associated with the absence of univocal geochemical and geophysical magma movement signs from multi-parametric data acquired by the dense monitoring system of the caldera (Vanorio et al., 2005; Battaglia et al., 2008).

Changes in the deformation rate during the last ten years correlate with the changes in seismicity rate and maximum magnitude of recorded events. Specifically, since 2020 there has been an acceleration of ground uplift in the Campi Flegrei caldera, reaching in September 2023 a rate of 1-1.5 cm/month (Figures 1c, 1d), accompanied by an exponential increase in the earthquake rate to about 1000 events per month (Figure 1d). Most of the earthquakes in the caldera occur at depths shallower than 3 km, with a near-elliptical distribution as from the reference catalogue of INGV (National Institute for Geophysics and Volcanology; Figure 1a). Most events have duration magnitude Md $\leq$ 1, though starting in early 2023 there is a general increase of the average magnitude per month, including several events with Md $\geq$ 3 and a largest, Md 4.2 earthquake, occurred on September 27, 2023.

The occurrence of five Md 3.6+ earthquakes during the period August 18 – October 2, widely felt in the Campi Flegrei and Napoli metropolitan area, raised a great concern in the population and civil protection authorities about the earthquake risk related to the volcanic activity. Given the high-density urbanization of the area, it is therefore important to understand the impact, including potential damage, to buildings and infrastructures caused by the repeated occurrence of small to moderate, shallow-depth events generated by the accelerating ground uplift.

In this study, we obtained multi-scale, high-precision relocations of the ongoing seismicity, allowing to identify, with unprecedented detail, the location and geometry of the activated structures during this crisis in the central area of the caldera. We used these new results along with mapped surface faults and fractures and other geophysical information to better understand the mechanics of earthquake faulting in relation to the caldera resurgence and other volcanic phenomena, with the aim of identifying zones where future, larger magnitude earthquake can potentially occur.

2 Event Dataset

We used P and S arrival-times from the earthquake catalogue provided by the INGV – Osservatorio Vesuviano from 01/01/2014 to 14/11/2023 (Figure 1a), available at https://terremoti.ov.ingv.it/gossip/flegrei. Phase arrivals and associated relative uncertainties and event duration magnitudes Md from only the fully located events in the catalogue (8292 earthquakes) are used. For the selected events, Md ranges between -1.1 and 4.2, with the Md 4.2 event (2023-09-27 01:35:34) having the largest number of phase arrival times (18 P and 6 S picks). Events with lower magnitude (Md < 2) typically show 6 to 10 P, 2 to 4 S arrival times. We also extracted arrival times from 18 stations of the INGV national network (yellow and red triangles in Figure 1a), located within 15 km from the catalogue epicentres. For the same set of events, we also recovered vertical component waveforms from 9 velocimetric stations available on EIDA portal (https://eida.ingv.it; red triangles in Figure 1a). We extracted waveforms in the time window from 10 s before to 45 s after the event origin time and decimated the traces to a sampling frequency of 50 Hz.

3. High-precision earthquake location

We obtained multi-scale, high-precision earthquake locations with a new procedure based on the NonLinLoc location algorithm (Lomax et al., 2000; Lomax et al., 2014; NLL hereafter) which produces an a-posterior probability density function (PDF) in 3D space for hypocentre location. The new procedure, NLL-SSST-coherence (NLL-SC), combines source-specific, station travel-time corrections (SSST) with stacking of PDFs, probabilistic location for nearby events based on waveform similarity (Lomax and Savvaidis, 2022; Lomax and Henry, 2023).

In a first relocation step, NLL-SC iteratively develops SSST corrections on collapsing length scales

(Richards-Dinger and Shearer, 2000; Lomax and Savvaidis, 2022), which can greatly improve, multi-scale relative location accuracy and clustering of events. In a second relocation step, NLL-SC reduces finer scale relative errors by consolidating information across locations based on waveform coherency between the events (Lomax and Savvaidis, 2022). This procedure is based on the concept that if the waveforms for two events at a station are very similar (e.g., have high coherency) up to a given frequency, then the distance between the two events is small relative to the wavelength corresponding to that frequency (e.g., Geller and Mueller, 1980; Poupinet et al., 1984). In this study we apply NLL-SC up to a frequency of 10 Hz, giving improved relative location accuracy down to ~100 m scale. See the Supporting Information (Text S1) for more details on the location procedure, velocity model (Figure S2) and processing parameters used in this study.

4. Results

The high-precision NLL-SC locations delineate several clusters and alignments of seismicity produced during the ongoing unrest at Campi Flegrei. Most of the seismicity concentrates in the shallow region around the Solfatara-Pisciarelli area (cyan-green dots in Figure 2). Here, epicenters define an ~1x1 km, horseshoe-shaped structure, opened and deepening toward the northeast beneath the Agnano Plain, and slightly larger than the ~0.5 km diameter of the Solfatara crater. Smaller-scale seismicity clusters, with a typical size of 100-300m, occur south and southwest of Solfatara, along the coast toward the center of Pozzuoli and the location of RITE station. This area has been active since 2014 (Figure 3), although the seismicity has intensified during the last three years.

The most recent magnitude Md 3.6+ events, except for the largest magnitude Md 4.2 earthquake, also occurred in the Solfatara-Pisciarelli area, beneath the horseshoe-shaped seismicity, at depths between 2 and 3.5 km. Northwest of the Solfatara crater, seismicity depicts a E-W trending, 1.5-2.0 km long structure composed of event cluster at depths comparable to that of the major events in the Solfatara.

Southeastward, off the coast of Bagnoli, a ~1km long, sub-vertical alignment trending just E of N is well defined by the relocated seismicity. This alignment contains the largest recorded event (Md 4.2), which ruptured an area of 800-1200 m^2, according to the calculated source radius (Figure S1 of Supporting Information). Further offshore to the southwest the seismicity occurs at greater depths, down to ~4 km, and forming a WNW oriented alignment offshore of Bacoli, and a N-S

198 alignment off the coast of Monte Nuovo. Overall, this seismicity forms an elliptical shape,
199 punctuated by the lineations and clusters containing the larger magnitude (Md > 3) events.
200

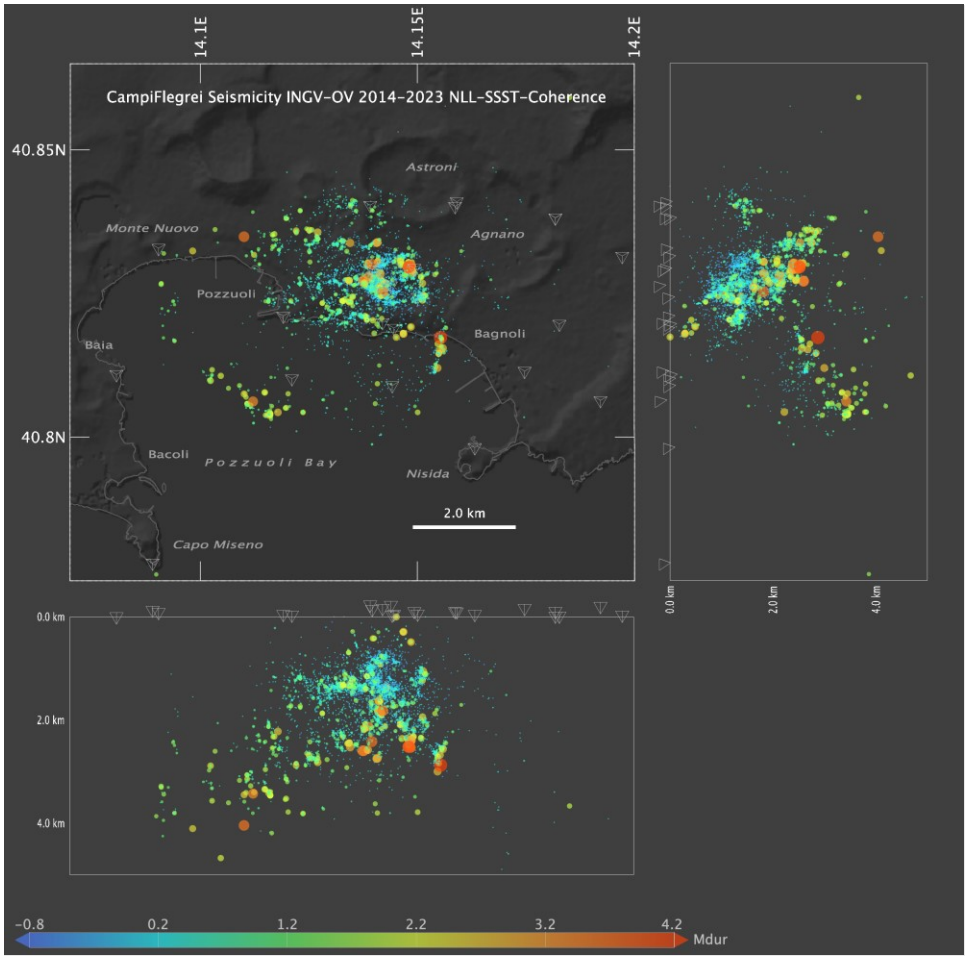

201

202 **Figure 2:** Relocated NLL-SC seismicity 2014-2023. Circles – color coded according to the magnitude
203 duration - show earthquakes with duration magnitude Md ≥ -1.0 and ellipsoid major axis ≤ 2.0 km (7212
204 of 8274 total relocated events); symbol size is proportional to magnitude. Tetrahedrons show subsets of
205 stations from Figure 1a used for relocation.
206

207 The evolution of the seismicity over time (Figures 1d and 3) shows an increasing of the number of
208 events and maximum magnitude. Moreover, while in the period 2014-2019 seismicity occurred at
209 shallow depths (most of these events have depth < 2 km) and concentrated in the Solfatara-
210 Pisciarelli area, during 2019-2023 the seismicity deepens, extends offshore and increases in
211 maximum magnitude. During the last two years (2022-2023), the seismicity spreads to a larger
212 area, forming the elliptical, ring-like structure, extending from inland north of Solfatara

213 southwards through Bagnoli, eastwards towards Bacoli and northward towards Monte Nuovo.
214
215 **5. Discussion**
216 The precisely located NLL-SC seismicity delineates the fault zones activated during the ongoing
217 seismic crisis at Campi Flegrei (Figure 2) with greater detail as compared to the raw bulletin dataset
218 (Figure 1a). Accurate delineation of the structures enables an improved interpretation of the fault
219 activation mechanisms in relation with the spatial stress variability and concentration as caused by
220 the extended ground uplift phenomenon. The multi-scale station corrections and waveform-
221 coherence based hypocenter consolidation of NLL-SC achieves a location precision of 100 m or
222 less, which is necessary to image faulting structures in a complex, multi-kilometer scale volcanic
223 environment such as Campi Flegrei.
224 The spatiotemporal activation of shallow crustal volumes during 2014-2023 within the inner
225 caldera is shown by the relocated seismicity (Figure 3 and Supporting Information Video S1).
226 In the period 2014-2019 a low seismicity rate is observed (Figure 1c), mostly characterized by
227 small magnitude ($Md < 2$) events occurring at depths shallower than about 3 km (Figure 3). These
228 events are located within a 1-2 km radius from the Solfatara crater which hosts, together with the
229 adjacent Pisciarelli fumarolic field, the most vigorous hydrothermal activity in the caldera
230 (Chiodini et al., 2017; Tamburello et al., 2019).
231 Overall, the variations in rate and magnitude of seismicity over time occur simultaneously with
232 changes in ground uplift rate of growth as observed at the station RITE in mid-2017, mid-2020
233 and end of 2022 (Figures 1c, d). Uplift velocity rather than cumulative uplift seems to control
234 localized seismicity production with the progressive activation of relatively long fracture zones at
235 the margin of the uplifting resurgent dome (Bevilacqua et al., 2022; Tramelli et al., 2022).
236 The spatial distribution of relocated seismicity (Figure 4) allows for an integrated geo-structural
237 interpretation based on recent evidence and reconstructions. The near-elliptical shape formed by
238 the seismicity since 2021 (Figure 4) resembles that of the 1982-84 crisis, whose seismicity
239 distribution has been related to a central collapsed portion of the caldera in studies (Barberi et al.,
240 1991; De Natale et al., 2006), which also considered results of gravity and magnetic surveys (Rosi
241 and Sbrana, 1987).
242

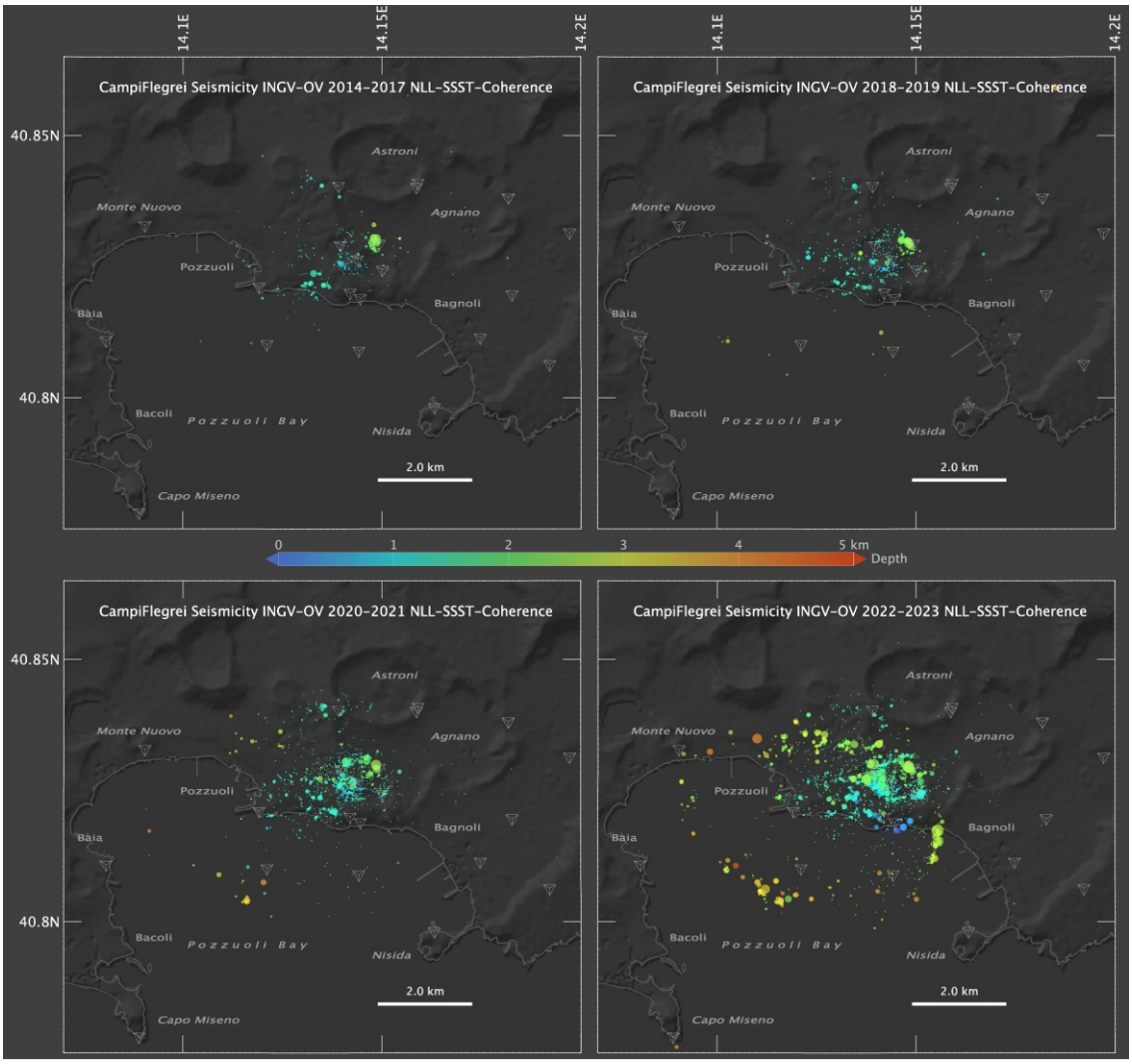

Figure 3: Spatiotemporal evolution of the seismicity in periods 2014-2017, 2018-2019, 2020-2021 and 2022-2023. Circles show earthquakes with magnitude Md ≥ -1.0 and ellipsoid major axis ≤ 2.0 km; symbol size is proportional to magnitude. Tetrahedrons show stations used for relocation.

However, this hypothesis is contradicted by the geological evidence of a nested caldera structure (e.g., Orsi et al., 1996; Di Vito et al., 1999). Only a part of the relocated seismicity, occurring in the offshore sector (Feature A in Figure 4), is compatible with the caldera ring fault zone (e.g., Sacchi et al., 2014; Steinmann et al., 2018). In a recent interpretation of high-resolution, seismic reflection profiles offshore of the caldera, Natale et al. (2022b) present evidence for a composite, ring-fault zone. This fault zone has an inner-ring confining from the west to the south-east the resurgent dome area, this latter being affected by a dense array of high-angle NE-SW to NNE-SSW trending, km-size collapse faults that cut the shallow marine sediments (Natale et al., 2020).

Several authors differentiate the inner-ring structure from the medial and outer ring fault systems, whose expression at depth matches well the annular high-P-velocity, high-density body, imaged by the 2001 active seismic tomography experiment and identified as the buried rim of the caldera (Zollo et al., 2003; Judenherc and Zollo, 2004; Battaglia et al., 2008; Dello Iacono et al., 2009). Only the deepest offshore seismicity, between 3-5 km depth, appears to fit and approximate the downward propagation of the south-western inner ring fault (Figure 4a, f), where the most frequent dip angles are between 60-80° (Natale et al., 2022b). This is consistent with a steep (~70°) inward-dipping fault structure that justifies the 1.2 km spatial gap between the surface projection of the mapped inner-ring fault and the 4 km deep epicenter locations. The focal mechanism solution (see Supporting Information, Text S3) is consistent in terms of strike and dip of the nodal plane, although with right-lateral kinematics (event 6 in Figure 4).

Activation of the Baia section (Feature B in Figure 4) of the inner ring fault (Vitale and Natale, 2023) can explain the seismicity off the coast of Monte Nuovo (between 3-5 km depth), where underwater high-temperature hydrothermal manifestations occur (Di Napoli et al., 2016). The more scattered and shallower seismicity could be related to high-angle faults as detailed in Natale et al. (2022b), also involved by hot fluid uprise (Carlino et al., 2016).

Of particular interest is the near N-S trending sub-vertical fault structure just offshore La Pietra (Feature C in Figure 4), generating the largest magnitude (Md 4.2) recorded event up to now during the crisis, and overall producing earthquakes between 2-4 km depth. This structure has not been identified previously as it lies in a region where no deep-penetrating seismic reflection profiles are available. From spectral modelling of seismic displacement records the average seismic moment and corner frequency of the event indicate a southward rupture extending over ~800-1200 m^2 (Figure and Text S1 in Supporting Information), which is consistent with the area filled by nearby seismicity (Figure 4), and the calculated focal mechanism (event 7 in Figure 4). However, given the near-vertical dip angle and related hypocenter uncertainty, this fault structure could be dipping to the east or to the west.

The offshore La Pietra fault structure illuminated by the relocated seismicity, represents a new seismogenic feature in the caldera as compared to the 1982-84 crisis (e.g., Orsi et al., 1999). This feature falls in the eastern portion of the near-elliptical seismicity pattern (Figure 4). The stress drop estimated for the Md 4.2 event (2-3 MPa) in this structure is large in relation to the depth of

the structure, suggesting a high strength of rocks in the shallow caprock or underlying basement (Vanorio and Kanitpanyacharoen, 2015).

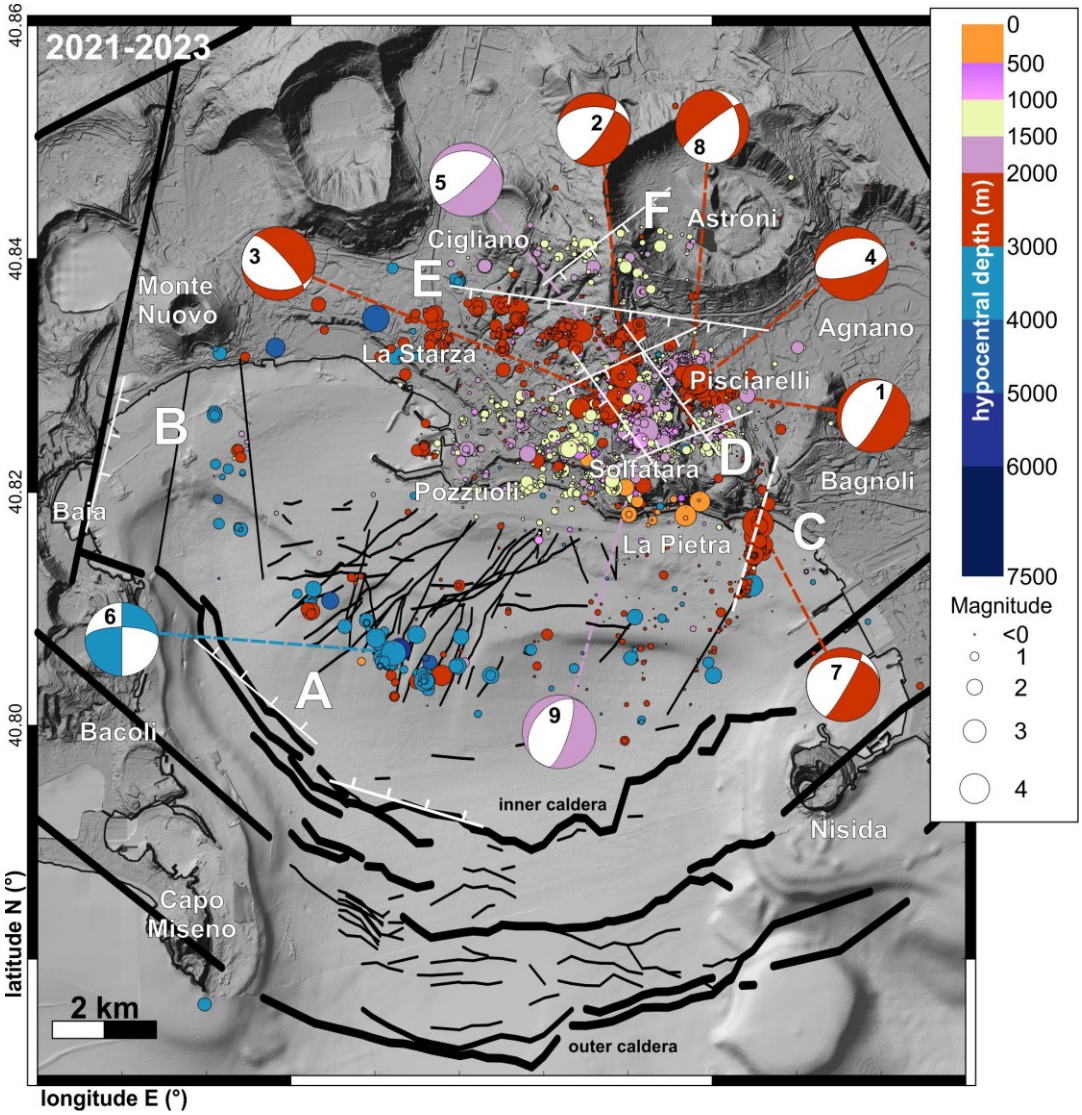

Figure 4. Simplified structural map showing the relationship between the epicentral distribution of relocated seismicity in the 2021-2023 period with the elliptical pattern and the main volcano-tectonic structures known in literature. Focal mechanisms solutions for selected 2023 Md>3 events are shown (details in Figure S3), with their color coded by depth.

Despite the moderate size of the event, the high stress drop acting over a small size asperity may be responsible for large peaks in the observed ground motion amplitudes (maximum recorded PGA of 0.3 g; see http://shakemap.ingv.it/shake4/ archive.html).

In the Solfatara area (Figure 4, Feature D) the relocated seismicity matches well several fault arrays mapped in the surface and subsurface geology. These fault arrays are related to the maar-diatreme structure of Solfatara crater, whose polygonal shape is due to the presence of main NW-SE and NE-SW faults, locally cross-cut by smaller E-W faults (Diamanti et al., 2022), and also exposed at Pisciarelli fumarole field within the western rim of Agnano caldera (Isaia et al., 2021). Hence, the horseshoe distribution of seismicity deepening eastward (Isaia et al., 2021) fits well the presence of such array faults at depth, which significantly affects the hydrothermal circulation in the area (Troiano et al., 2019). The calculated focal mechanisms (Figure 4 and Supporting Information Text S3) show nodal planes consistent with the mapped structures, as they are mainly NE-SW trending (events 1, 2, 5 and 8), and subordinately E-W trending (event 4) and NW-SE (event 3).

An approximately E-W trending fault bounds the distribution of the relocated seismicity NE of the Solfatara crater (Figure 4, Feature E), on which a series of spatially and temporally correlated seismicity bursts occurred between 2 and 3 km depths. This structure corresponds to a south-dipping normal fault with a left-lateral component, with noticeable surface expression in Agnano and Cigliano as recently depicted in Natale et al. (2023) and corroborated by structural field data by Diamanti et al. (2022). The bursts of seismicity occur along a ca. 6 km-long structure, that to the west reaches La Starza marine terrace (Vitale et al., 2019), representing the northern border of elliptical seismicity.

The NE-SW seismicity alignment (Figure 4, Feature F) in the Astroni might be associated with pressurized fluids moving along a NE-SW faults within the shallow (1-1.5 km) portion of the hydrothermal system (Isaia et al., 2022), where increased hydrothermal activity has been detected, as corroborated by microgravity data (Young et al., 2020).

5. Conclusions

The general elliptical distribution of the ongoing seismicity at Campi Flegrei caldera is mainly driven by the stress concentration causative effect of a bell-shaped ground deformation pattern with fracture zones that appear coherent with the ones activated during the 1982-84 unrest in shape and location (Scarpa et al., 2022). However, new sectors have been activated during the present unrest, at the eastern boundary, where the largest Md 4.2 event was caused by a km-size rupture within the shallow (3 km) volcanic sedimentary layer. We found that several structures delineated

by the ongoing seismicity have correspondence in the geological shallow fault record, whose formation was not related to the same volcanic-tectonic process (i.e., dome resurgence), but rather generated by other, more energetic processes such volcano-tectonic collapses, magma intrusion and migration.

In general, the stress changes caused by the ongoing uplift of the central caldera appear to concentrate on weaker pre-existing structures that are reactivated by small-to-moderate, sub-kilometric fractures. All the Md 3.6+ earthquake ruptures, apart from the largest Md 4.2 event, have nucleated along segments of the complex SW-NE and SE-NW fault system array at the margins of the Solfatara crater. As for the Md 4.2 event, the evidence for relatively high stress-drops and average slip (2-3 MPa, 3-5 cm see Supporting Information) suggests a possible effect of fluid-driven, pore-pressure increase at these faults that could favor the development of larger size fractures.

Considering the size of the structures mapped in this study and the stress drop estimated for the main event (Text S1 of Supporting Information), these faults can accommodate earthquakes of moment magnitude up to 5.0, both beneath the Solfatara and offshore, south of Pozzuoli, significantly increasing the hazard in the area.

References

Barberi, F., Cassano, E., La Torre, P., & Sbrana, A. (1991). Structural evolution of Campi Flegrei caldera in light of volcanological and geophysical data. *Journal of volcanology and geothermal research*, 48(1-2), 33-49.

Battaglia, J., Zollo, A., Virieux, J., & Dello Iacono, D. (2008). Merging active and passive data sets in traveltime tomography: The case study of Campi Flegrei caldera (Southern Italy). *Geophyiscal Prospecting*, 56, 555–573. https://doi.org/10.1111/j.1365-2478.2007.00687.x

Bevilacqua, A., Isaia, R., Neri, A., Vitale, S., Aspinall, W. P., Bisson, M., Flandoli, F., Baxter, P.J., Bertagnini, A., Esposti Ongaro, T., Iannuzzi, E., Pistolesi, M., & Rosi, M. (2015). Quantifying volcanic hazard at Campi Flegrei caldera (Italy) with uncertainty assessment: 1. Vent opening maps. *Journal of Geophysical Research: Solid Earth*, 120(4), 2309-2329.

Bevilacqua, A., Neri, A., De Martino, P., Isaia, R., Novellino, A., Tramparulo, F. D. A., & Vitale, S. (2020). Radial interpolation of GPS and leveling data of ground deformation in a resurgent caldera: application to Campi Flegrei (Italy). *Journal of Geodesy*, 94, 1-27.

Bevilacqua, A., De Martino, P., Giudicepietro, F., Ricciolino, P., Patra, A., Pitman, E. B., Bursik, M., Voight, B., Flandoli, F., Macedonio, G., & Neri, A. (2022). Data analysis of the unsteadily accelerating GPS and seismic records at Campi Flegrei caldera from 2000 to 2020. *Scientific reports*, 12(1), 19175.

Bianco, F., Caliro, S., De Martino, P., Orazi, M., Ricco, C., Vilardo, G., Aquino, I., Augusti, V., Avino, R., Bagnato, E., Brandi, G., Caputo, A., Carandente, A., Chiodini, G., Cuoco, E., D'Alessandro, A., Dolce, M., Guardato, S., Minopoli, C., Sansivro, F., Santi, A., Scarpato, G., Tramelli, A., & Castellano, M. (2022). The permanent monitoring system of the Campi Flegrei caldera, Italy. In Campi Flegrei: A Restless Caldera in a Densely Populated Area (pp. 219-237). *Berlin, Heidelberg*. Springer Berlin Heidelberg.

Bonasia, V., Pingue, F., & Scarpa, R. (1984). A fluid-filled fracture as possible mechanism of ground deformation at Phlegraean Fields, Italy, *Bullettin of Volcanology*, 47(2), 313–320.

Bonafede, M. (1991). Hot fluid migration: An efficient source of ground deformation: Application to the 1982–1985 crisis at Campi Flegrei-Italy, *Journal of Volcanology and Geothermal Research,* 48, 187–198.

Carlino, S., Mirabile, M., Troise, C., Sacchi, M., Zeni, L., Minardo, A., Caccavale, M., Daranyi, V., & De Natale, G. (2016). Distributed-temperature-sensing using optical methods: a first application in the offshore area of Campi Flegrei caldera (Southern Italy) for volcano monitoring. *Remote Sensing*, 8(8), 674.

Charlton, D., Kilburn, C., & Edwards, S. (2020). Volcanic unrest scenarios and impact assessment at Campi Flegrei caldera, Southern Italy. *Journal of Applied Volcanology*, 9, 1-26.

Chiodini, G., Selva, J., Del Pezzo, E., Marsan, D., De Siena, L., D'Auria, L., Bianco, F., Caliro, S., De Martino, P., Ricciolino, P., & Petrillo, Z. (2017). Clues on the origin of post-2000 earthquakes at Campi Flegrei caldera (Italy). *Scientific reports*, 7(1), 4472.

De Natale, G., Troise, C., Pingue, F., Mastrolorenzo, G., Pappalardo, L., Battaglia, M., & Boschi, E. (2006). The Campi Flegrei caldera: unrest mechanisms and hazards. *Geological Society, London, Special Publications*, 269(1), 25-45.

Del Gaudio, C., Aquino, I., Ricciardi, G.P., Ricco, C., & Scandone, R. (2010). Unrest episodes at Campi Flegrei: a reconstruction of vertical ground movements during 1905-2009*Journal of Volcanology and Geothermal Research*, 195, 48–56.

390 Dello Iacono, D., Zollo, A., Vassallo, M., Vanorio, T., & Judenherc, S. (2009). Seismic images
391 and rock properties of the very shallow structure of Campi Flegrei caldera (southern Italy).
392 *Bulletin of Volcanology* 71, 275–284. https://doi.org/10.1007/s00445-008-0222-1.
393 Diamanti, R., Camanni, G., Natale, J., & Vitale, S. (2022). A gravitational origin for volcano-
394 tectonic faults in the Campi Flegrei caldera (southern Italy) inferred from detailed field
395 observations. *Journal of Structural Geology*, 161, 104671.
396 Di Napoli, R., Aiuppa, A., Sulli, A., Caliro, S., Chiodini, G., Acocella, V., Ciraolo, G., Di Vito,
397 M. A., Interbartolo, F., Nasello, C., & Valenza, M. (2016). Hydrothermal fluid venting in
398 the offshore sector of C ampi F legrei caldera: A geochemical, geophysical, and
399 volcanological study. *Geochemistry, Geophysics, Geosystems*, 17(10), 4153-4178.
400 Di Vito, M. A., Isaia, R., Orsi, G., Southon, J. D., De Vita, S., d'Antonio, M., Pappalardo, L., &
401 Piochi, M. (1999). Volcanism and deformation since 12,000 years at the Campi Flegrei
402 caldera (Italy). *Journal of Volcanology and Geothermal Research*, 91(2–4), 221–246.
403 https://doi.org/10.1016/S0377-0273(99)00037-2
404 Di Vito, M. A., Acocella, V., Aiello, G., Barra, D., Battaglia, M., Carandente, A., Del Gaudio, C.,
405 de Vita, S., Ricciardi, G. P., Ricco, C., Scandone, R., & Terrasi, F. (2016). Magma transfer
406 at Campi Flegrei caldera (Italy) before the 1538 AD eruption, *Scientific Reports*, 6(1), 1–
407 9.
408 Gaeta, F. S., Peluso, F., Arienzo, I., Castagnolo, D., De Natale, G., Milano, G., Albanese, C. &
409 Mita, D. G. (2003). A physical appraisal of a new aspect of bradyseism: The miniuplifts.
410 *Journal of Geophysical Research: Solid Earth*, 108(B8).
411 Geller, R. J., & Mueller, C. S. (1980). Four similar earthquakes in central California. *Geophysical*
412 *Research Letters*, *7*(10), 821–824. https://doi.org/10.1029/GL007i010p00821
413 Isaia, R., Di Giuseppe, M. G., Natale, J., Tramparulo, F. D. A., Troiano, A., & Vitale, S. (2021).
414 Volcano-tectonic setting of the Pisciarelli fumarole field, Campi Flegrei caldera, southern
415 Italy: Insights into fluid circulation patterns and hazard scenarios. *Tectonics*, 40(5),
416 e2020TC006227.
417 Isaia, R., Di Giuseppe, M. G., Troiano, A., Avino, R., Caliro, S., Santi, A., & Vitale, S. (2022).
418 Structure and present state of the Astroni Volcano in the Campi Flegrei caldera in Italy
419 based on multidisciplinary investigations. *Geochemistry Geophysics Geosystems*, 23(12),
420 e2022GC010534.

Judenherc, S., & Zollo, A. (2004). The Bay of Naples (southern Italy): Constraints on the volcanic structures inferred from a dense seismic survey. *Journal of Geophysical Research: Solid Earth*, 109(B10).

Krischer, L., Megies, T., Barsch, R., Beyreuther, M., Lecocq, T., Caudron, C., & Wassermann, J. (2015). ObsPy: A bridge for seismology into the scientific Python ecosystem. Computational Science & Discovery, 8(1), 014003.

Lomax, A., Virieux, J., Volant, P., & Berge-Thierry, C. (2000). Probabilistic Earthquake Location in 3D and Layered Models. In C. H. Thurber & N. Rabinowitz (Eds.), *Advances in Seismic Event Location*, 18, 101–134. Springer Netherlands. https://doi.org/10.1007/978-94-015-9536-0_5

Lomax, A., Michelini, A., & Curtis, A. (2014). Earthquake Location, Direct, Global-Search Methods. In R. A. Meyers (Ed.), *Encyclopedia of Complexity and Systems Science* (pp. 1–33). Springer New York. https://doi.org/10.1007/978-3-642-27737-5_150-2

Lomax, A., & Savvaidis, A. (2022). High-Precision Earthquake Location Using Source-Specific Station Terms and Inter-Event Waveform Similarity. *Journal of Geophysical Research: Solid Earth*, *127*(1), e2021JB023190. https://doi.org/10.1029/2021JB023190

Lomax, A., & Henry, P. (2023). Major California faults are smooth across multiple scales at seismogenic depth. *Seismica*, *2*(1), Article 1. https://doi.org/10.26443/seismica.v2i1.324.

Lomax, A., & Scotto di Uccio, F. (2023). Relocated event catalog for 2014-2023 seismicity at Campi Flegrei [Data set]. *Zenodo*. https://doi.org/10.5281/zenodo.10259822

Lomax, A. (2023). NLL-SC processing parameters for the relocation of the 2014-2023 Campi Flegrei seismicity [Data set]. *Zenodo*. https://doi.org/10.5281/zenodo.10260849

Macedonio, G., Giudicepietro, F., D'Auria, L., & Martini, M. (2014). Sill intrusion as a source mechanism of unrest at volcanic calderas. *Journal of Geophysical Reseacrh: Solid Earth*, 119, 3986–4000. https://doi.org/10.1002/2013JB010868

McNutt, S. R., Scarpa, R., & Tilling, R. I. (1996). Monitoring and mitigation of volcano hazards. In *Berlin, Federal Republic of Germany, Springer-Verlag, Ch. Seismic monitoring and eruption forecasting of volcanoes: a review of the state-of-the-art and case histories* (pp. 99-146)

Natale, J., Ferranti, L., Marino, C., & Sacchi, M. (2020). Resurgent dome faults in the offshore of the Campi Flegrei caldera (Pozzuoli Bay, Campania): preliminary results from high-resolution seismic reflection profiles. *Bollettino di Geofisica Teorica ed Applicata*, 61(3).

Natale, J., Ferranti, L., Isaia, R., Marino, C., Sacchi, M., Spiess, V., Steinmann, L., & Vitale, S. (2022a). Integrated on-land-offshore stratigraphy of the Campi Flegrei caldera: new insights into the volcano-tectonic evolution in the last 15 kyr. *Basin Research* 34 (2), 855–882.

Natale, J., Camanni, G., Ferranti, L., Isaia, R., Sacchi, M., Spiess, V., Steinmann, L., & Vitale, S. (2022b). Fault systems in the offshore sector of the Campi Flegrei caldera (southern Italy): implications for nested caldera structure, resurgent dome, and volcano-tectonic evolution. *Journal of Structural Geology*. 163:104723. https://doi.org/10.1016/j.jsg.2022.104723

Natale, J., Vitale, S., Repola, L., Monti, L., & Isaia, R. (2023). Digital Surface Model Generated from Vintage Aerial Photographs: a glance at the pre-urbanization morphology of the active Campi Flegrei caldera. *Geomorphology*. *Under review.*

Nespoli, M., Tramelli, A., Belardinelli, M. E., & Bonafede, M. (2023). The effects of hot and pressurized fluid flow across a brittle layer on the recent seismicity and deformation in the Campi Flegrei caldera (Italy). *Journal of Volcanology and Geothermal Research*, 443, 107930.

Orsi, G., D'Antonio, M., de Vita, S., & Gallo, G. (1992). The Neapolitan Yellow Tuff, a large-magnitude trachytic phreatoplinian eruption: eruptive dynamics, magma withdrawal and caldera collapse. *Journal of Volcanology and Geothermal Research*, 53(1-4), 275-287.

Orsi, G., De Vita, S., & Di Vito, M. (1996). The restless, resurgent Campi Flegrei nested caldera (Italy): constraints on its evolution and configuration. *Journal of Volcanology and Geothermal Research*, 74(3-4), 179-214.

Orsi,G. (2022) Volcanic and Deformation History of the Campi Flegrei Volcanic Field, Italy in Orsi, G., D'Antonio, M., Civetta, L. (Eds.), Campi Flegrei: A Restless Caldera in a Densely Populated Area, Active Volcanoes of the World. Springer Berlin Heidelberg, Berlin, Heidelberg. https://doi.org/10.1007/978-3-642-37060-1

Osservatorio Vesuviano, INGV (2023) Monthly Bulletin on Campi Flegrei,

Poupinet, G., Ellsworth, W. L., & Frechet, J. (1984). Monitoring velocity variations in the crust using earthquake doublets: An application to the Calaveras Fault, California. *Journal of*

Geophysical Research: Solid Earth, *89*(B7), 5719–5731. https://doi.org/10.1029/JB089iB07p05719

Reasenberg, P. A (1985) FPFIT, FPPLOT, and FPPAGE : Fortran computer programs for calculating and displaying earthquake fault-plane solutions, U.S. Geol. Surv. Open-File Rep.,pp: 85-739

Richards-Dinger, K. B., & Shearer, P. M. (2000). Earthquake locations in southern California obtained using source-specific station terms. *Journal of Geophysical Research: Solid Earth*, *105*(B5), 10939–10960. https://doi.org/10.1029/2000JB900014

Rosi, M., & Sbrana, A. (1987). Phlegrean fields. *Quaderni de la ricerca scientifica*, 9(114).

Sacchi, M., Pepe, F., Corradino, M., Insinga, D. D., Molisso, F., & Lubritto, C. (2014). The Neapolitan Yellow Tuff caldera offshore the Campi Flegrei: Stratal architecture and kinematic reconstruction during the last 15 ky. *Marine Geology*, 354, 15-33.

Scarpa,R. Bianco, F.,Capuano,P. Castellano,M., D'Auria,L.,Di Lieto,B. and Romano P. (2022) Historic unrest of the Campi Flegrei Caldera, Italy in Orsi, G., D'Antonio, M., Civetta, L. (Eds.), Campi Flegrei: A Restless Caldera in a Densely Populated Area, Active Volcanoes of the World. Springer Berlin Heidelberg, Berlin, Heidelberg. https://doi.org/10.1007/978-3-642-37060-1

Silleni, A., Giordano, G., Isaia, R., & Ort, M. H. (2020). The magnitude of the 39.8 ka Campanian Ignimbrite eruption, Italy: method, uncertainties and errors. *Frontiers in Earth Science*, 8, 543399.

Steinmann, L., Spiess, V., & Sacchi, M. (2018). Post-collapse evolution of a coastal caldera system: Insights from a 3D multichannel seismic survey from the Campi Flegrei caldera (Italy*). Journal of Volcanology and Geothermal Research*, 349, 83-98.

Tamburello, G., Caliro, S., Chiodini, G., De Martino, P., Avino, R., Minopoli, C., Carandente, A., Rouwet, D., Aiuppa, A., Costa, A, Bitetto, M., Giudice, D., Francofonte, V., Ricci, T., Sciarra, A., Bagnato, E., & Capecchiacci, F. (2019). Escalating CO2 degassing at the Pisciarelli fumarolic system, and implications for the ongoing Campi Flegrei unrest. *Journal of Volcanology and Geothermal Research*, 384, 151-157.

Tilling, R. I. (2008). The critical role of volcano monitoring in risk reduction. *Advances in Geosciences*, 14, 3-11.

Todesco, M. (2021). Caldera's Breathing: Poroelastic Ground Deformation at Campi Flegrei (Italy). *Frontiers in Earth Science* 9, 702665. https://doi.org/10.3389/feart.2021.702665

Tramelli, A., Giudicepietro, F., Ricciolino, P., & Chiodini, G. (2022). The seismicity of Campi Flegrei in the contest of an evolving long term unrest. *Scientific reports*, 12(1), 2900.

Troiano, A., Isaia, R., Di Giuseppe, M. G., Tramparulo, F. D. A., & Vitale, S. (2019). Deep Electrical Resistivity Tomography for a 3D picture of the most active sector of Campi Flegrei caldera. *Scientific reports*, 9(1), 15124.

Troise, C., De Natale, G., Schiavone, R., Somma, R., & Moretti, R. (2019). The Campi Flegrei caldera unrest: Discriminating magma intrusions from hydrothermal effects and implications for possible evolution. *Earth-Science Reviews* 188, 108–122. https://doi.org/10.1016/j.earscirev.2018.11.007

Young, N., Isaia, R., & Gottsmann, J. (2020). Gravimetric constraints on the hydrothermal system of the Campi Flegrei caldera. *Journal of Geophysical Research: Solid Earth*, 125(7), e2019JB019231.

Vanorio, T., J. Virieux, P. Capuano, & G. Russo (2005), Three-dimensional seismic tomography from P wave and S wave microearthquake travel times and rock physics characterization of the Campi Flegrei caldera. *Journal of Geophysical Research: Solid Earth*, 110, B03201, doi:10.1029/2004JB003102.

Vanorio, T., & Kanitpanyacharoen, W. (2015). Rock physics of fibrous rocks akin to Roman concrete explains uplifts at Campi Flegrei Caldera. *Science*, 349(6248), 617-621.

Vitale, S., Isaia, R., Ciarcia, S., Di Giuseppe, M. G., Iannuzzi, E., Prinzi, E. P., Tramparulo, F.D.A., & Troiano, A. (2019). Seismically induced soft-sediment deformation phenomena during the volcano-tectonic activity of Campi Flegrei caldera (southern Italy) in the last 15 kyr. *Tectonics*, 38(6), 1999-2018.

Vitale, S., & Natale, J. (2023). Combined volcano-tectonic processes for the drowning of the Roman western coastal settlements at Campi Flegrei (southern Italy). *Earth Planets and Space*, 75(1), 1-15.

Woo, J.Y.L., & Kilburn, C.R.J. (2010). Intrusion and deformation at Campi Flegrei, southern Italy: Sills, dikes, and regional extension. *Journal of Geophysical Research: Solid Earth* 115, 2009JB006913. https://doi.org/10.1029/2009JB006913

Zollo, A., Judenherc, S., Auger, E., D'Auria, L., Virieux, J., Capuano, P., Chiarabba, C., De Franco, R., Makris, J., Michelini, A., & Musacchio, G. (2003). Evidence for the buried rim of Campi Flegrei caldera from 3-d active seismic imaging. *Geophysical Research Letters* 30, 2003GL018173. https://doi.org/10.1029/2003GL018173

Zollo, A., Maercklin, N., Vassallo, M., Dello Iacono, D., Virieux, J., & Gasparini, P. (2008), Seismic reflections reveal a massive melt layer feeding Campi Flegrei caldera, *Geophysical Research Letters* 35, L12306, doi:10.1029/2008GL034242.

Open Research

The phase arrival times used in this study are available at the INGV-Osservatorio Vesuviano bulletin database, at the link https://terremoti.ov.ingv.it/gossip/index.html. Information is available per event. Seismic waveforms can be accessed through EIDA portal (https://eida.ingv.it/it/), network code IV. Relocated event catalog is available on zenodo at the link: https://doi.org/10.5281/zenodo.10259822 (Lomax and Scotto di Uccio, 2023). All earthquake relocations were performed with NonLinLoc (Lomax et al., 2000; Lomax et al., 2014; http://www.alomax.net/nlloc; https://github.com/alomax/NonLinLoc). SeismicityViewer (http://www.alomax.net/software) was used for 3D seismicity analysis and plotting, ObsPy (Krischer et al., 2015), (http://obspy.org) for waveform processing and coherence calculations. NLL-SC processing parameters for the relocation of the seismicity are available on zenodo at the link: https://doi.org/10.5281/zenodo.10260849 (Lomax, 2023).

Supporting Information summary

Text S1 to S3

Figure S1 to S3

Table S1

Movie S1 to S3

References in Supporting Information

Brune, J. N. (1970). Tectonic stress and the spectra of seismic shear waves from earthquakes. *Journal of Geophysical Research*, *75*(26), 4997–5009. https://doi.org/10.1029/JB075i026p04997

572 Keylis-Borok, V. (1959). On estimation of the displacement in an earthquake source and of source
573 dimensions. *Annals of Geophysics*, *12*(2).
574 Judenherc, S., Zollo, A., 2004. The bay of Naples (southern Italy: Constraints on thevolcanic
575 structures inferred from a dense seismic survey. J. Geophys. Res. Solid Earth109 (B10).
576 https://doi.org/10.1029/2003JB002876.
577 Matoza, R. S., Shearer, P. M., Lin, G., Wolfe, C. J., & Okubo, P. G. (2013). Systematic relocation
578 of seismicity on Hawaii Island from 1992 to 2009 using waveform cross correlation and
579 cluster analysis. *Journal of Geophysical Research: Solid Earth*, 118(5), 2275-2288.
580 Podvin, P., & Lecomte, I. (1991). Finite difference computation of traveltimes in very contrasted
581 velocity models: a massively parallel approach and its associated tools. *Geophysical*
582 *Journal International*, 105(1), 271-284.
583 Reasenberg, P. A. (1985). FPFIT, FPPLOT, and FPPAGE: Fortran computer programs for
584 calculating and displaying earthquake fault-plane solutions. *US Geol. Surv. Open-File*
585 *Rep.*, 85-739.
586 Supino, M., Festa, G., & Zollo, A. (2019). A probabilistic method for the estimation of earthquake
587 source parameters from spectral inversion: Application to the 2016-2017 Central Italy
588 seismic sequence. *Geophysical Journal International*, *218*(2), 988–1007.
589 https://doi.org/10.1093/gji/ggz206
590 Tarantola, A. (2004). *Inverse Problem Theory and Methods for Model Parameter Estimation*.
591 Tramelli, A., Godano, C., Ricciolino, P., Giudicepietro, F., Caliro, S., Orazi, M., ... & Chiodini,
592 G. (2021). Statistics of seismicity to investigate the Campi Flegrei caldera unrest. *Scientific*
593 *Reports*, 11(1), 7211.
594 Trugman, D. T., & Shearer, P. M. (2018). Strong correlation between stress drop and peak ground
595 acceleration for recent M 1–4 earthquakes in the San Francisco Bay area. *Bulletin of the*
596 *Seismological Society of America*, 108(2), 929-945.
597 Waldhauser, F., & Ellsworth, W. L. (2000). A double-difference earthquake location algorithm:
598 Method and application to the northern Hayward fault, California. *Bulletin of the*
599 *seismological society of America*, 90(6), 1353-1368.
600 Zhou, H. W. (1994). Rapid three-dimensional hypocentral determination using a master station
601 method. *Journal of Geophysical Research: Solid Earth*, 99(B8), 15439-15455.
602